

AD-A155 558

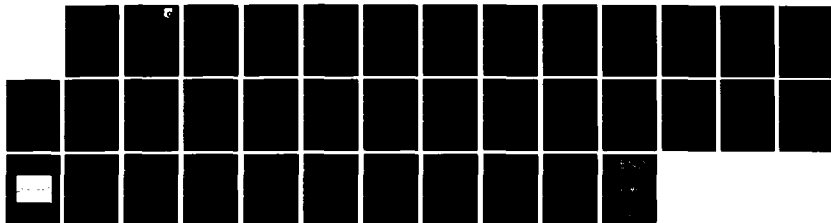
DETECTION OF EXCITED STATES BY LASER-INDUCED
FLUORESCENCE(U) NATIONAL BUREAU OF STANDARDS BOULDER CO
QUANTUM PHYSICS DIV H TISCHER ET AL. APR 85
AFWAL-RR-84-2113 MIPR-FV1455-83-N0632

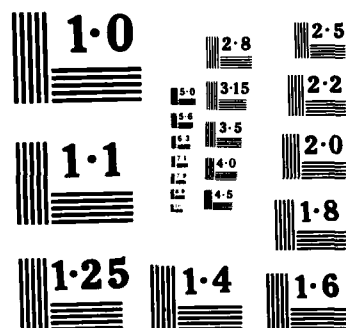
1/1

UNCLASSIFIED

F/G 7/4

NL





NATIONAL BUREAU OF STANDARDS
MICROCOPY RESOLUTION TEST CHART

AFWAL-TR-84-2113



DETECTION OF EXCITED STATES BY LASER-INDUCED FLUORESCENCE

H. TISCHER and A. V. PHELPS

QUANTUM PHYSICS DIVISION
U. S. BUREAU OF STANDARDS
BOULDER, CO 80303

April 1985

FINAL REPORT FOR PERIOD OCTOBER 1982 - SEPTEMBER 1984

Approved for public release; distribution unlimited

AERO PROPULSION LABORATORY
AIR FORCE WRIGHT AERONAUTICAL LABORATORIES
AIR FORCE SYSTEMS COMMAND
WRIGHT-PATTERSON AIR FORCE BASE, OHIO 45433

DTIC FILE COPY

JUN 23 1985

NOTICE

When Government drawings, specifications, or other data are used for any purpose other than in connection with a definitely related Government procurement operation, the United States Government thereby incurs no responsibility nor any obligation whatsoever; and the fact that the government may have formulated, furnished, or in any way supplied the said drawings, specifications, or other data, is not to be regarded by implication or otherwise as in any manner licensing the holder or any other person or corporation, or conveying any rights or permission to manufacture use, or sell any patented invention that may in any way be related thereto.

This report has been reviewed by the Office of Public Affairs (ASD/PA) and is releasable to the National Technical Information Service (NTIS). At NTIS, it will be available to the general public, including foreign nations.

This technical report has been reviewed and is approved for publication.

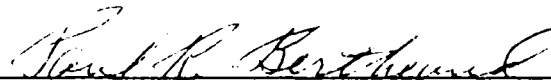


Research Physicist
Plasma Physics Group
Aerospace Power Division
Aero Propulsion Laboratory

FOR THE COMMANDER



JAMES D. REAMS
Chief, Aerospace Power Division
Aero Propulsion Laboratory



Chief, Power Components Branch
Aerospace Power Division
Aero Propulsion Laboratory

"If your address has changed, if you wish to be removed from our mailing list, or if the addressee is no longer employed by your organization please notify AFWAL/PMOC-3 W-PAFB, OH 45433 to help us maintain a current mailing list".

Copies of this report should not be returned unless return is required by security considerations, contractual obligations, or notice on a specific document.

UNCLASSIFIED

SECURITY CLASSIFICATION OF THIS PAGE (When Data Entered)

REPORT DOCUMENTATION PAGE		READ INSTRUCTIONS BEFORE COMPLETING FORM
1. REPORT NUMBER AFWAL-TR-84-2113	2. GOVT ACCESSION NO. 10-4155 558	3. RECIPIENT'S CATALOG NUMBER
4. TITLE (and Subtitle) DETECTION OF EXCITED STATES BY LASER-INDUCED FLUORESCENCE		5. TYPE OF REPORT & PERIOD COVERED Final Oct. 82 - Sept. 84
		6. PERFORMING ORG. REPORT NUMBER
7. AUTHOR(s) H. Tischer and A. V. Phelps		8. CONTRACT OR GRANT NUMBER(s) MIPR FY1455-83-N0632 MIPR FY1455-84-N0631 MIPR FY1455-84-N0602
9. PERFORMING ORGANIZATION NAME AND ADDRESS Quantum Physics Division U.S. Bureau of Standards Boulder, CO 80303		10. PROGRAM ELEMENT, PROJECT, TASK AREA & WORK UNIT NUMBERS P.E. 61102F Proj. 2301, Task 51 Work Unit 24
11. CONTROLLING OFFICE NAME AND ADDRESS Aero Propulsion Laboratory (AFWAL/POOC) AF Wright Aeronautical Laboratories (AFSC) Wright-Patterson Air Force Base, OH 45433		12. REPORT DATE April 1985
		13. NUMBER OF PAGES 28
14. MONITORING AGENCY NAME & ADDRESS (if different from Controlling Office)		15. SECURITY CLASS. (of this report) Unclassified
		15a. DECLASSIFICATION/DOWNGRADING SCHEDULE
16. DISTRIBUTION STATEMENT (of this Report) Approved for public release; distribution unlimited.		
17. DISTRIBUTION STATEMENT (of the abstract entered in Block 20, if different from Report)		
18. SUPPLEMENTARY NOTES		
19. KEY WORDS (Continue on reverse side if necessary and identify by block number) hydrogen, electrons, radiation, excitation coefficient, fluorescence, excited states		
20. ABSTRACT (Continue on reverse side if necessary and identify by block number) Laser absorption techniques have been developed for the measurement of densities of $H_2(C^3P_u)$ metastable densities in H_2 electrical discharges. Using this technique and a modulated discharge we have found that the metastable density is proportional to discharge current density for current densities up to $10 A/cm^2$. By using a pulsed laser to destroy the metastables we have obtained preliminary measurements of the metastable lifetime as a function of H_2 density.		

DD FORM 1 JAN 73 1473

EDITION OF 1 NOV 65 IS OBSOLETE

UNCLASSIFIED

SECURITY CLASSIFICATION OF THIS PAGE (When Data Entered)

PREFACE

This work was performed in the Quantum Physics Division, U.S. Bureau of Standards, at the Joint Institute for Laboratory Astrophysics under MIPR FY1455-83-N0632, MIPR FY 1455-84-N0631 and MIPR FY1455-84-N0602. The work was performed during the period October 1983 through September 1984 under Project 2301 Task S1, Work Unit 24. The Air Force contract manager was Dr. Alan Garscadden, Energy Conversion Branch, Air Force Wright Aeronautical Laboratories, Aero Propulsion Laboratory, WPAFB, OH 45433.

APPROVED	
FOR	
DISSEMINATION	
UNCLASSIFIED	
DATE	
BY	
DTIC	
AD	
ELC	
A-1	



TABLE OF CONTENTS

SECTION	PAGE
I. INTRODUCTION	1
II. PREVIOUS RESEARCH	2
III. DIAGNOSTIC TECHNIQUES	6
IV. H_2 $c^3\Pi_u$ METASTABLE KINETICS	12
A. Pulsed discharge experiments	12
B. Current dependence of metastable density	14
C. Pressure dependence	16
D. High time resolution experiments	16
E. Models of H_2 excited state behavior	21
V. CONCLUSIONS	25
REFERENCES	27

LIST OF ILLUSTRATIONS

FIGURE	PAGE
1. Lower excited states of triplet system of H_2 . The diagonal lines show some of the radiative transitions of interest in our experiment.....	3
2. Lower rotational states of the $v=1$ vibrational state of the H_2 ($c^3\Pi_u$) state and some of the rotational levels of the $v=1$ state of some of the $n=3$ states.....	4
3. Scan of absorption signal for $573 < \lambda < 598$ nm. The symbols used to identify the lines are the vibrational level of the $c^3\Pi_u$ state, the rotational transition, and the upper electronic state.....	7
4. Scans of laser induced fluorescence signals from the $c^3\Pi_u$ state. a) LIF using filter peaked at 170 nm. b) LIF using photo-multiplier sensitive to $100 < \lambda < 200$ nm.....	10
5. Pulsed discharge emission and laser absorption transient by $H_2(c^3\Pi_u)$ metastables.....	13
6. Peak absorption signal vs peak discharge current for $H_2(c^3\Pi_u)$ metastables.....	15
7. Schematic of apparatus used in high time resolution absorption measurements.....	17
8. Overall transient absorption waveform showing effects during discharge pulse -- first and third arrows -- and metastable depletion caused by laser pulse -- center arrow.....	19
9. Expanded absorption waveform showing recovery of $c^3\Pi_u$ ($N=1$, $v=2$) metastable population and exponential fit to data.....	20

10. Decay constants (upper two curves) and relative amplitudes of UV emission (lower curve) for collisionally coupled $c^3\Pi_u$ and $a^3\Sigma_g^+$ states of H_2 . The solid lines are calculated neglecting collision coupling while the dashed line is calculated using the maximum collision rate coefficient consistent with the emission data shown by the circular points. The square points show our preliminary decay constant measurements..... 22

LIST OF TABLES

TABLE	PAGE
1. Observed absorption wavelengths and intensities of $H_2(c^3\Pi_u)$ metastables.....	8

SECTION I

INTRODUCTION

The overall objective of the research described in this report is to develop diagnostics and models required for measurement and prediction of the properties of electrical discharges in molecular gases. Such discharges are of interest to the Air Force because of their utility in devices such as high power switches, negative ion sources, lasers, and radio frequency discharge processing and because of their role in phenomena such as lightning and corona. The research program includes a) the development and application of laser fluorescence and absorption techniques to the measurement of excited state densities in electric discharges, b) the measurement of the properties of the excited states of importance in molecular discharges of current interest, c) the application of various diagnostic techniques to the determination of the characteristics of moderate current density, transient electrical discharges, and d) the quantitative comparison of these results with appropriate discharge models.

During the past year we have been concerned with the development and application of the laser diagnostic techniques to the measurement of the properties of the $c^3\Pi_u$ metastable state of H_2 . The properties of metastable H_2 are of current interest because of the use of discharges in H_2 as switching devices (thyatrons), as negative ion sources, and as infrared lasers.

Previous work on the $c^3\Pi_u$ state of H_2 is summarized in Sec. II. The diagnostic techniques being applied to the measurement of the properties of the $c^3\Pi_u$ state are discussed in Sec. III, while the techniques and results obtained thus far for the collisional destruction of the $c^3\Pi_u$ state are discussed in Sec. IV. Recommendations for future work are made in Sec. V.

SECTION II

PREVIOUS RESEARCH

The metastable nature of the $c^3\Pi_u$ state of H_2 has been the subject of many experimental¹⁻⁷ and theoretical⁸⁻¹⁰ investigations. Of particular interest for this investigation of the role of the $H_2(c^3\Pi_u)$ state in gas discharge devices are accurate measurements¹¹ of the wavelengths of spectral lines terminating on the $c^3\Pi_u$ state, measurements^{5,7} and theory⁷⁻⁹ showing the effects of predissociation and radiation on the $c^3\Pi_u$ state, calculations¹⁰ of the interactions of excited H_2 with ground state H_2 , and discussions of the role of the $c^3\Pi_u$ state in H_2 discharges¹²⁻¹⁵ and in astrophysics.¹⁶ Very recently, the properties of the predissociating levels of the $c^3\Pi_u$ state have been shown to be important in the operation of an infrared H_2 laser.¹⁷⁻¹⁸

The lower excited states of the triplet system of H_2 are shown in Fig. 1. The lowest rotational level $N=1$ of the $v=0$ vibrational level of the $c^3\Pi_u$ state lies 135 cm^{-1} below the lowest level ($N=0, v=0$) of the $a^3\Sigma_g^+$ state and so cannot radiate by an allowed dipole transition to the $b^3\Sigma_u^+$ state. The other relevant properties of the $H_2(c^3\Pi_u)$ state will be summarized with the aid of Fig. 2. Figure 2 shows the lower rotational levels of the $v=1$ vibrational states of the $c^3\Pi_u$ state and of some of the states with principal quantum number $n=3$. Also shown are the levels with + and - reflection symmetry which characterize the lambda doubling properties of the $^3\Pi_u$ states. Note that the splitting of the lambda doubled levels is too small to be observed in our experiments with Doppler limited resolution. Experiment¹ and theory⁸ show that the levels of + symmetry (designated $c^3\Pi^+$) have lifetimes against predissociation of about 10^{-9} s. The levels with - symmetry ($c^3\Pi^-$) have lifetimes^{1,13} against forbidden predissociation and radiation ranging from 1 ms

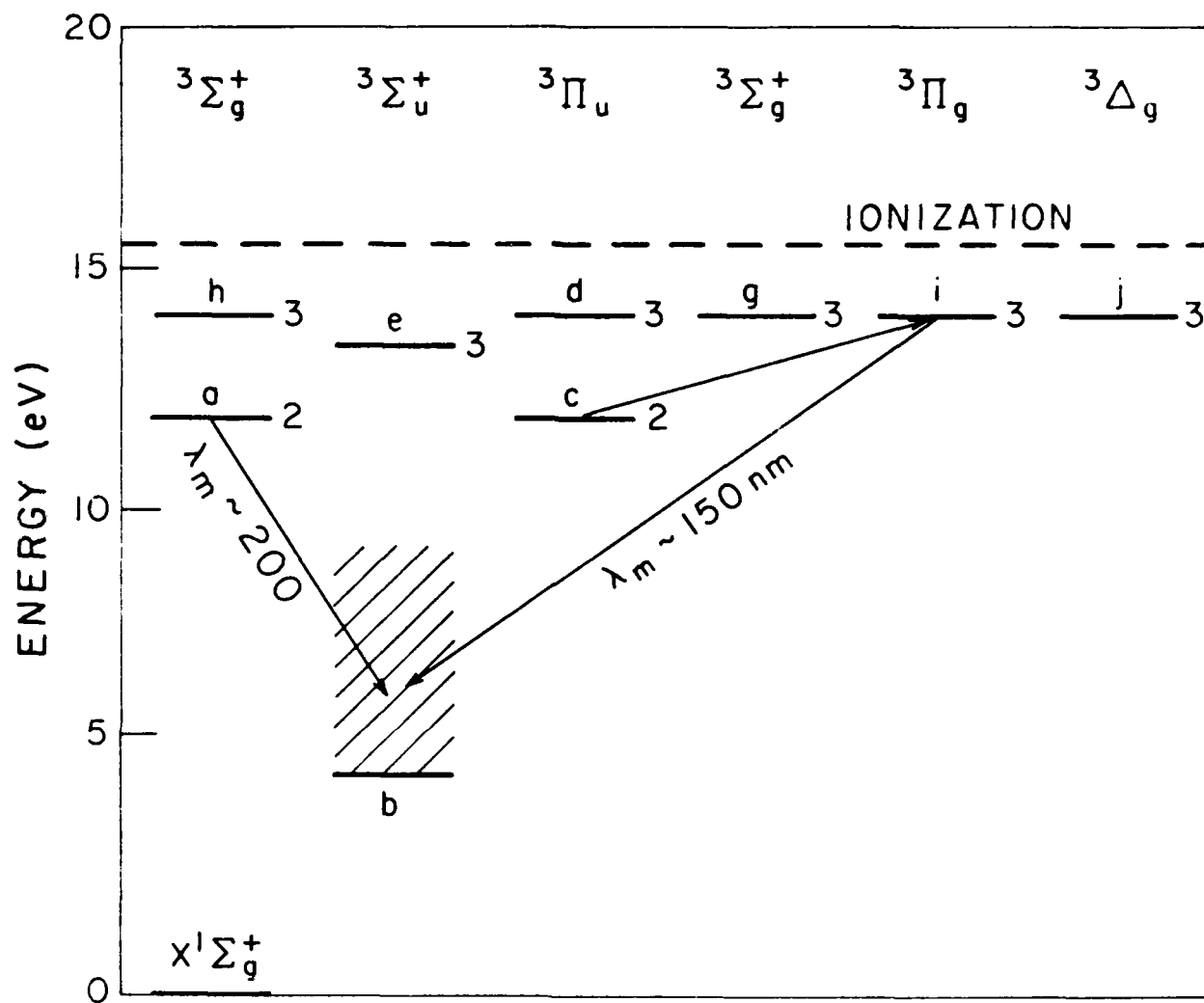


Figure 1. Lower excited states of triplet system of H_2 . The diagonal lines show some of the radiative transitions of interest in our experiment.

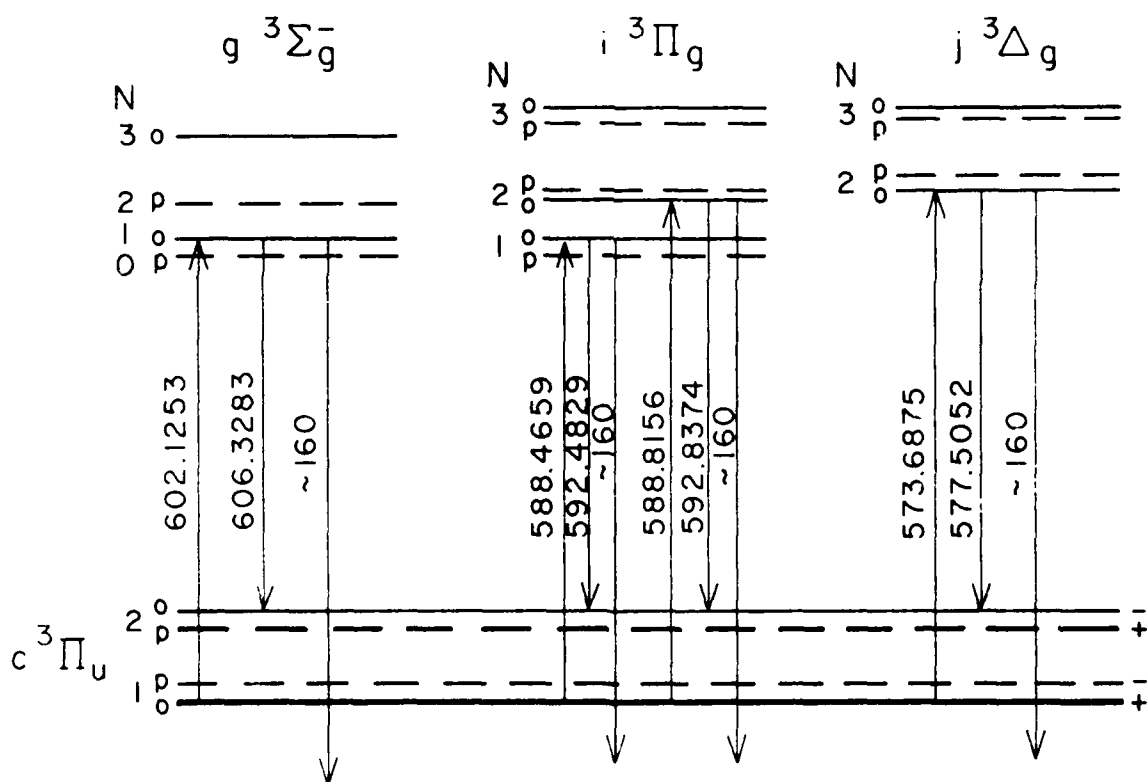


Figure 2. Lower rotational states of the $v=1$ vibrational state of the H_2 ($c \ ^3\Pi_u$) state and some of the rotational levels of the $v=1$ state of some of the $n=3$ states.

to 100 μ s, depending on the vibrational quantum number. These lifetimes are so long compared to the lifetimes observed in our experiment that the exact values are not important. Figure 2 shows that one possible route for collisional quenching of the Π^- levels is by rotational excitation or deexcitation with no change in ortho-para symmetry but with a change in inversion symmetry. Note that in spite of the small lambda doublet splitting, collisional or electric field^{4,10} mixing of the ortho- and para-levels is expected to be small, i.e., comparable with ortho-para conversion rate coefficients for H_2 .

Figure 2 also shows some of the radiative transitions of importance in the present experiments. As will be described in Sec. III we have observed a large number of transitions from levels of the $c^3\Pi_u^-$ state to higher states of H_2 . Unfortunately, very little information is available as to the radiative transition probabilities to be expected in the triplet system of H_2 . We would be particularly interested in data for the relative transition probabilities for the visible and UV transitions from the $n=3$ states to the $c^3\Pi$ and $b^3\Sigma$ states of H_2 .

SECTION III

DIAGNOSTIC TECHNIQUES

The laser diagnostic techniques which we have been testing for use with H_2 discharges are laser absorption, laser induced fluorescence (LIF), optogalvanic detection, and laser induced quenching. By far the most successful has been the laser absorption technique. Figure 3 shows a portion of a scan of the absorption signal produced by a H_2 discharge operating at a current density of 35 mA/cm^2 at a density of $2 \times 10^{22} \text{ m}^{-3}$. The laser line width for this set of data was estimated to be 30 GHz compared to a calculated Doppler width (FWHM) of 4.5 GHz, so that a better signal-to-noise ratio could be obtained by operating the laser in a single mode. More recently we have operated with a laser line width of about 7.5 GHz, but have not found it necessary to use single mode operation. Absorption signals of about 10% were obtained by operating the discharge with a peak current of about 5 A/cm^2 .

A total of 55 absorption lines were observed in the wavelength range from 574 to 614 nm. All except two of the lines were identified as H_2 lines using Dieke's compilation.¹² Forty-three lines were identified as originating on levels of the $c^3\Pi_u$ state. The relative value of the measured absorption and the associated quantum numbers of the rotational and vibrational levels for these transitions are listed in Table I. Six lines originate on levels of the $a^3\Sigma_g^+$ level and four are unidentified H_2 lines. Under some discharge conditions the two strongest lines are the sodium resonance lines, presumably caused by sodium released from the glass by the discharge. The strongest H_2 absorption lines originate on rotational levels with $N'' = 1$, as expected if $\Delta N = 0$ excitation by electrons is favored and if the line absorption

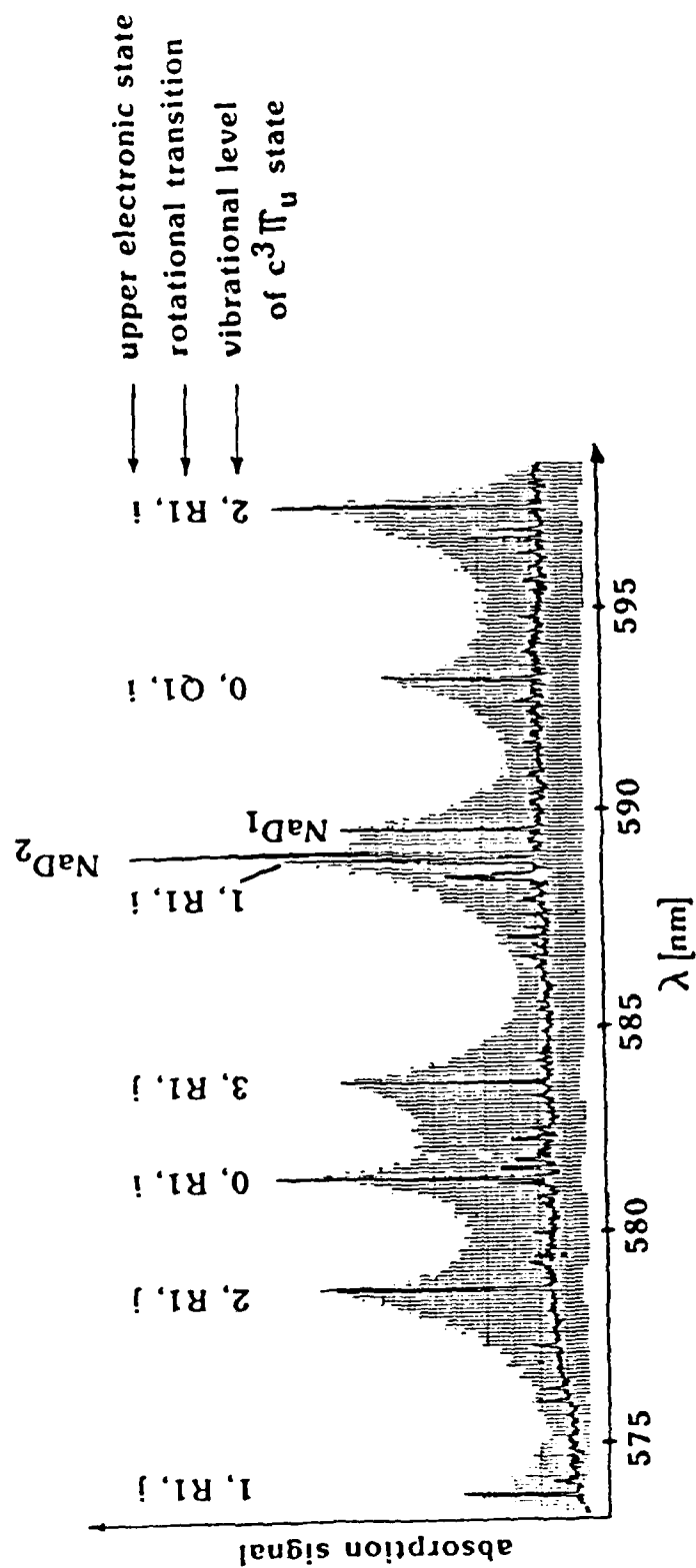


Figure 3. Scan of absorption signal for $573 < \lambda < 598$ nm. The symbols used to identify the lines are the vibrational level of the $c^3\Pi_u$ state, the rotational transition, and the upper electronic state.

Table I. Observed absorption wavelengths and intensities for $H_2(c^3n_u)$ metastables

Observed wavelength	Dicke ¹² wavelength	$v''=0$			$v''=1$			$v''=2$			$v''=3$		
		$N''=1$	$N''=2$	$N''=3$	$N''=1$	$N''=2$	$N''=3$	$N''=1$	$N''=2$	$N''=3$	$N''=1$	$N''=2$	$N''=3$
		ortho	para	ortho	ortho	para	ortho	ortho	para	ortho	ortho	para	ortho
613.4107	613.4284							1.4					
612.1328	612.1198							1.4					
610.0287	610.0199										0.9		
609.1018	609.0886						0.5						
607.8683	607.889										2.2		
607.1741	607.1568											0.5	
606.7601	606.7673												1.0
605.3403	605.3249					0.6				0.3			
604.5091	604.4641												
602.1216	602.1253				4.1								
600.3210	600.2811			0.4									
599.1772	599.1780												
598.8969	598.9224						0.5						
597.5449	597.5445							4.2		1.2			
596.9565	596.9682												
596.7378	596.7267									1.4			
596.3351	596.3462												
593.0738	593.1360	2.9	0.5										
592.5668	592.5380												
588.8708	588.8624*												0.8
588.8155	588.8156				6.4								
588.4510	588.4659					1.8							
588.3985	588.3938						2.1						
587.8362	587.8527									0.4			
587.1430	587.1619											0.3	
586.9013	586.9257												0.7
586.1774	586.1593*												
583.6118	583.6121										4.9		
583.2780	583.2764						0.3						
582.2144	582.2057								0.6				
581.7042	581.7070												
581.5020	581.4949									1.1		0.5	
581.2632	581.2602	7.7											
581.1869	581.1504		1.7										
578.6059	578.5768							8.1					

* $v''=1, N''=5$

coefficients are reasonably independent of level. Transitions originating on vibrational levels with v'' from 0 to 3 and with N'' from 1 to 5 are observed.

Examples of the laser induced fluorescence (LIF) signal from $c^3\Pi_u$ metastables² obtained by using UV sensitive photomultipliers are shown in Fig. 4. The discharge was operated at a H_2 density of $3 \times 10^{22} \text{ m}^{-3}$ with a square wave modulated current of 46 mA/cm^2 . The laser power was 400 mW and the photomultiplier output was measured using a synchronous detector. The upper trace shows data obtained using an interference filter peaking at 170 nm so as to eliminate discharge emission from the strongly excited³ singlet states of H_2 . This experiment yielded LIF only from vibrational levels of the $c^3\Pi_u$ state with $v''=0$. Since the Frank-Condon factors greatly favor $\Delta v = 0$, this observation suggests that only the $v'=0$ levels of states with principal quantum number $n=3$ are low enough in energy to result in the production of fluorescence continuum with wavelengths as long as 170 nm. The peak LIF signal was approximately 10^{-4} of the background emission.

LIF data taken with a photomultiplier and filter system sensitive to the wavelengths between 120 and 170 nm was used to obtain the signal shown in the lower trace of Fig. 2. In this case one observes LIF from levels of the $c^3\Pi_u$ state with $v''=0$ through,³ i.e., at the wavelengths of the stronger transitions observed in absorption. Note the poorer signal-to-noise ratio in the lower trace, presumably caused by the large intensity of singlet state emission from the discharge. The ratio of the LIF signal to the average discharge emission was about 2×10^{-5} . Since the LIF is a continuum the use of interference filters, etc. is not expected to significantly increase the LIF relative to noise. The large and slowly varying changes in background resulted from the drift of a striation past the observation window.

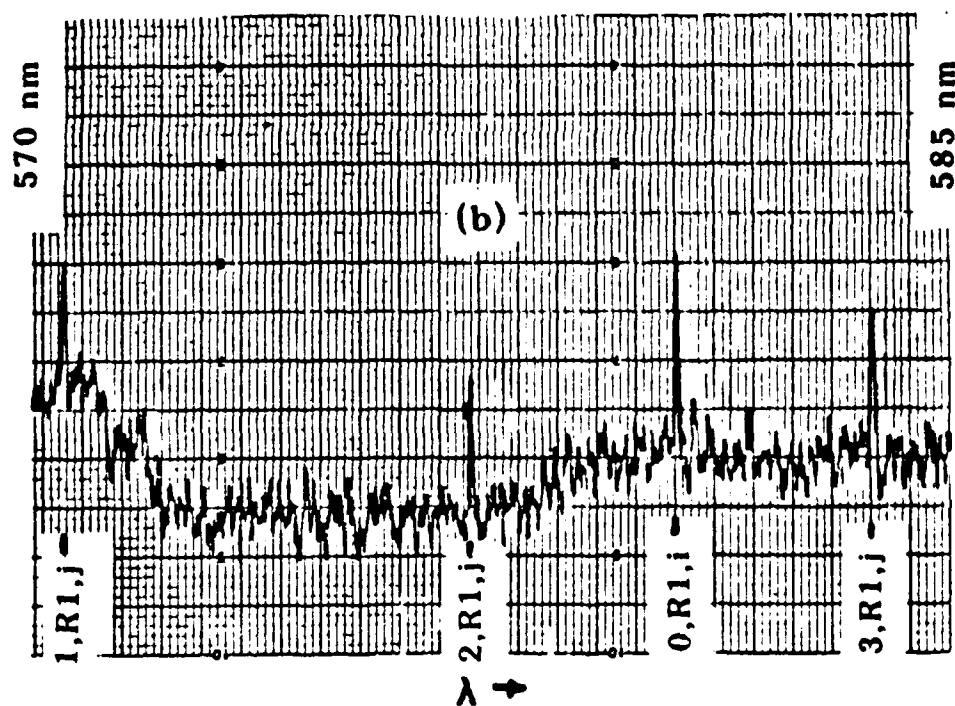
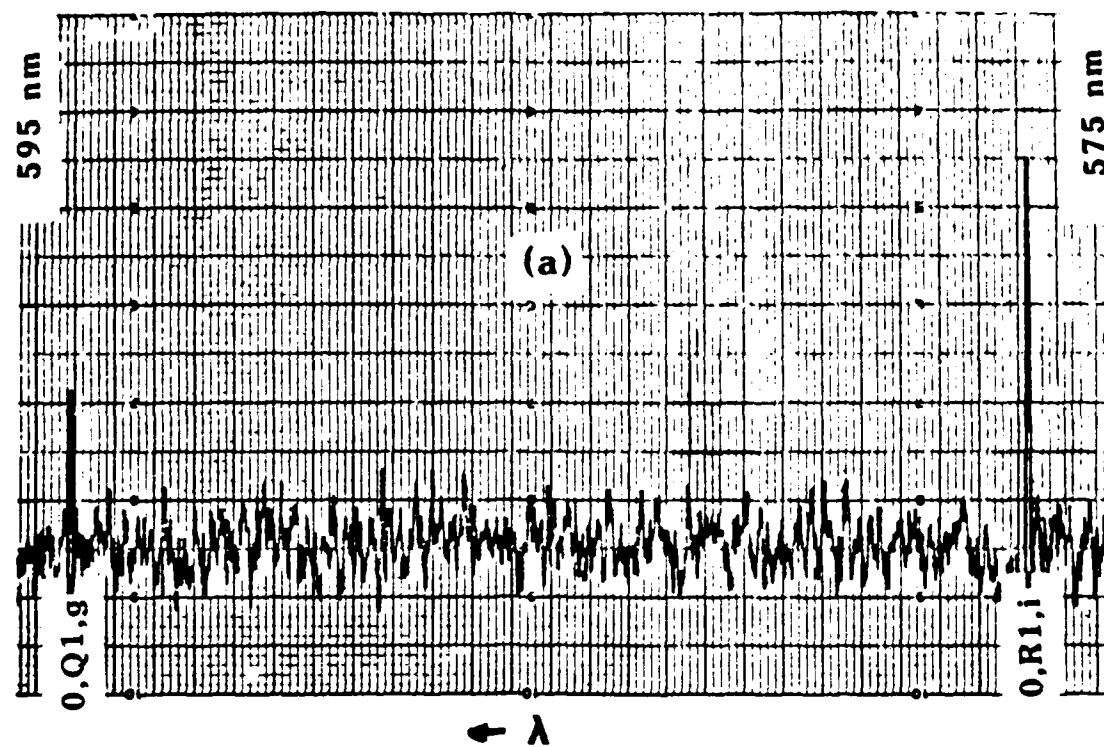


Figure 4. Scans of laser induced fluorescence signals from the $c^3\Pi_u$ state.
 a) LIF using filter peaked at 170 nm. b) LIF using photo-
 multiplier sensitive to $100 < \lambda < 200$ nm.

The optogalvanic detection technique¹⁹ was successfully used for 12 lines of the H₂ discharge in the wavelength range of 574 to 614 nm, but the signal-to-noise ratio was found to be too poor to be used for stabilization of our laser. We have therefore not developed this technique further.

SECTION IV

H_2 $c^3\Pi_u$ METASTABLE KINETICS

In view of the success of the laser absorption measurements of $c^3\Pi_u$ metastables, we are applying this technique to the measurement of the collisional destruction rate coefficients. On the basis of the information presented in Sect. III and of discussions with theoreticians we expected that the collisional destruction of the $c^3\Pi_u$ metastables by excitation transfer⁵ to other electronic states of H_2 would occur with a rate coefficient of less than about $2 \times 10^{-16} \text{ m}^3/\text{s}$, while that for destruction by rotational excitation and subsequent predissociation⁶ would be significantly less than the gas kinetic collision rate coefficient of about $4 \times 10^{-16} \text{ m}^3/\text{s}$. Thus, we expected that the lifetime would be of the order of microseconds at H_2 densities of 10^{22} m^{-3} . Accordingly, we attempted to measure the lifetime using pulsed discharges in H_2 lasting a fraction of a microsecond and using an absorption detection system having a response time of about 200 ns. This work is described in Sects. IV A and B. Our recent successful lifetime measurements are described in Sect. IV D.

A. Pulsed discharge experiments

Representative waveforms obtained with this arrangement are shown in Fig. 5. Here we see that the light emission from the discharge has an apparent full width at half maximum of about 250 ns, which is roughly what was expected from the discharge current waveform. Tests of the detector and amplifier chain with a high speed LED source showed that the response time of the detection system was in this same range. From the final decay of the absorption signal in Fig. 5 we estimated the lifetime for the $c^3\Pi_u$ metastables

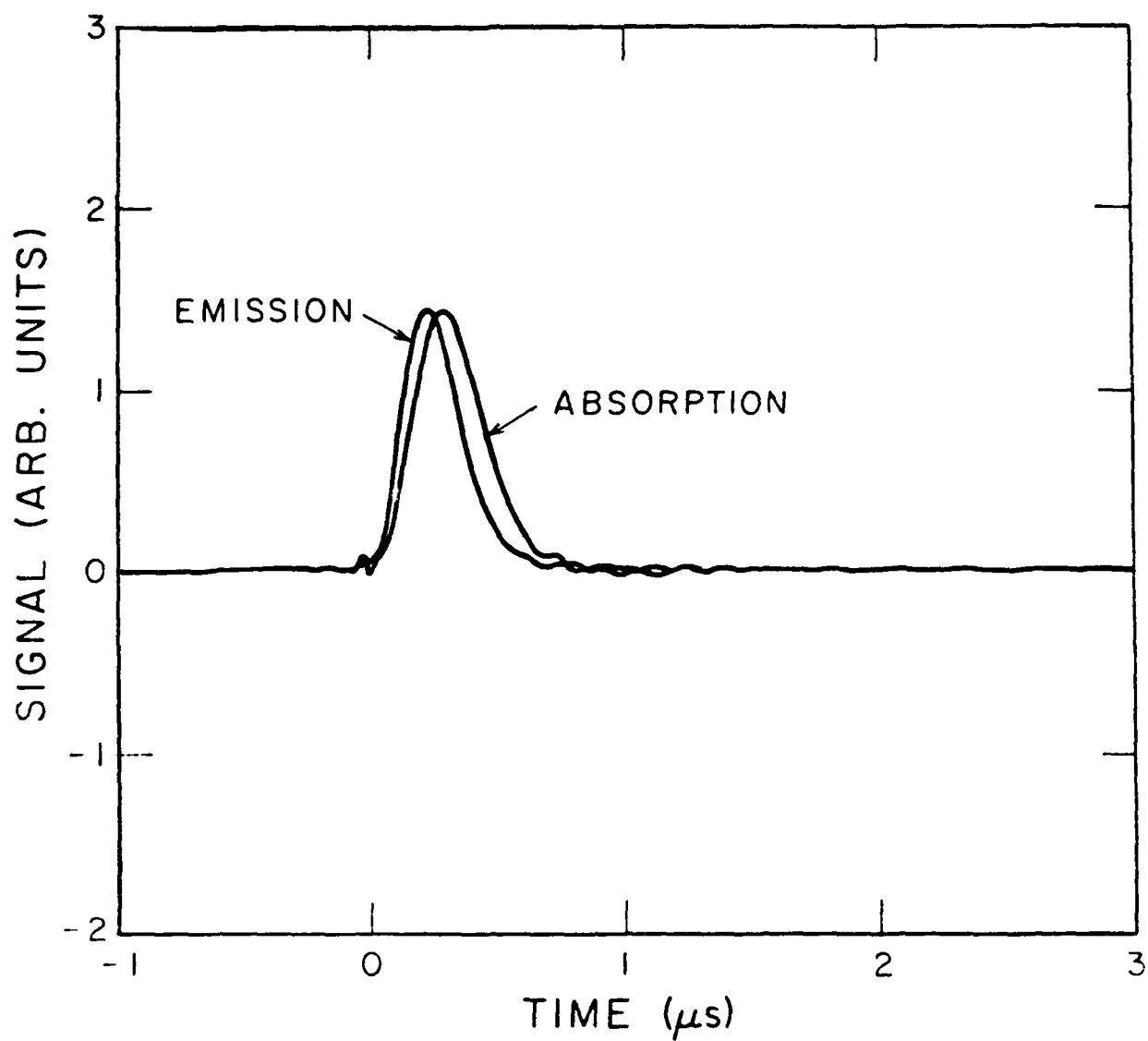


Figure 5. Pulsed discharge emission and laser absorption transient by $\text{H}_2(\text{c}^3\Pi_u)$ metastables.

to be less than about 150 ns. Since we were unable to operate the discharge in this short pulse mode at lower gas densities, we were unable to determine from this type of experiment whether the metastables were being destroyed in collisions with gas atoms or with electrons.

B. Current dependence of metastable density

In order to test for $c^3\Pi_u$ metastable destruction by electrons we measured the absorption signal over a wide range of discharge currents as shown in Fig. 6. This data shows that the peak absorption signal is approximately proportional to the discharge current for currents from 3×10^{-3} to 10 A/cm^2 , corresponding to electron densities from about 2×10^{15} to $6 \times 10^{18} \text{ m}^{-3}$. The H_2 density was $2.2 \times 10^{22} \text{ m}^{-3}$ and the discharge tube diameter was 5 mm. At this H_2 density our measurements show that the metastable lifetime is short compared to the discharge pulse length so that the peak absorption measurements can be interpreted using a quasi-steady-state model in which the production is balanced by the loss. If destruction by electrons were dominant at the higher currents we would expect the absorption signal to become independent of electron density and approximately independent of current. If the metastable destruction were by collisions with H_2 molecules we would expect the absorption to be proportional to electron density and therefore approximately proportional to current, as observed. We therefore tentatively conclude that the observed metastable destruction under the conditions of our experiments is due to collisions with H_2 and that from the data of Fig. 6 the rate coefficient for this destruction is greater than about $1.5 \times 10^{-15} \text{ m}^3/\text{s}$.

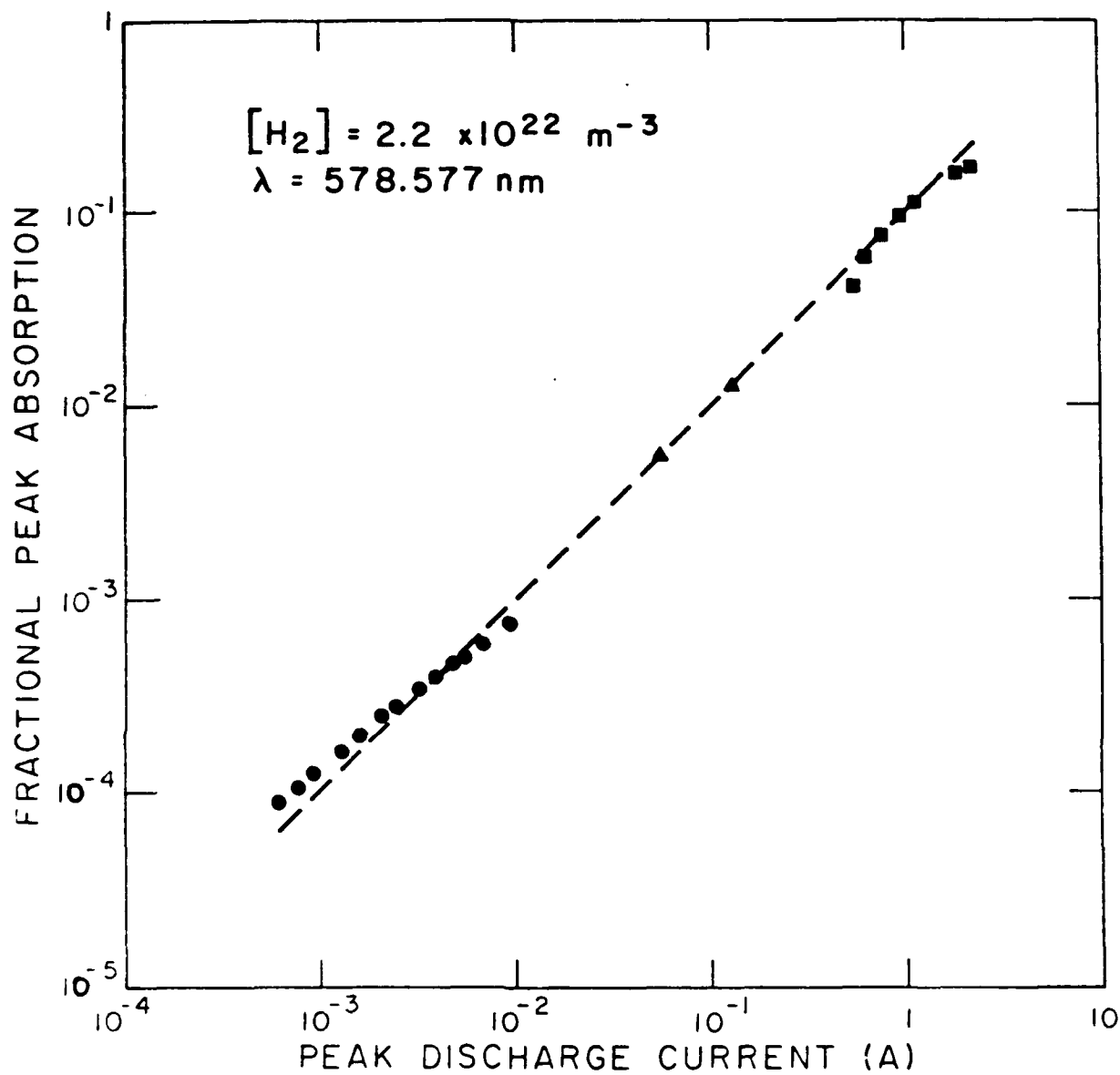


Figure 6. Peak absorption signal vs peak discharge current for $H_2(c^3\Pi_u)$ metastables.

C. Pressure dependence

We have also briefly examined the dependence of the peak absorption signal on the H_2 density at constant discharge current. The peak absorption was found to be independent of H_2 density for densities between 10^{22} and 10^{23} m^{-3} , as expected for destruction of $c^3\Pi_u$ by H_2 . However, at higher H_2 densities the absorption decreased with increasing H_2 density. This behavior is not understood.

D. High time resolution experiments

In view of the very large rate coefficient for $c^3\Pi_u$ metastable destruction, we have had to redesign our experiment to obtain much higher time resolution for the production and detection of changes in the metastable density. A schematic of the apparatus is shown in Fig. 7. A N_2 laser pumped, pulsed dye laser was used to destroy a portion of the metastables by excitation to higher states from which they can radiate to the $b^3\Sigma_u^+$ state. We measure this destruction and the subsequent recovery of metastable density by observing the absorption of the cw dye laser signal with a high speed photodiode and a fast transient digitizer. In the measurements made to date the pulsed dye laser is tuned to a wavelength of 597.5 nm shown in Fig. 2. This H_2 line was chosen because the absorption measured in Sec. III was large and because it is close to the strong optogalvanic line of Ne at 597.5 nm which can be used to indicate proper adjustment of the pulsed dye laser. The probe laser was set to the 578.6 nm line of H_2 . As shown in Fig. 2 these two H_2 lines have the same lower level.

In order to provide a high population of $c^3\Pi_u$ metastables the discharge was operated in the pulsed mode with a discharge length of about 4 μs , a current density of about 2 A/cm^2 , and a repetition rate of 30 Hz. The pulsed

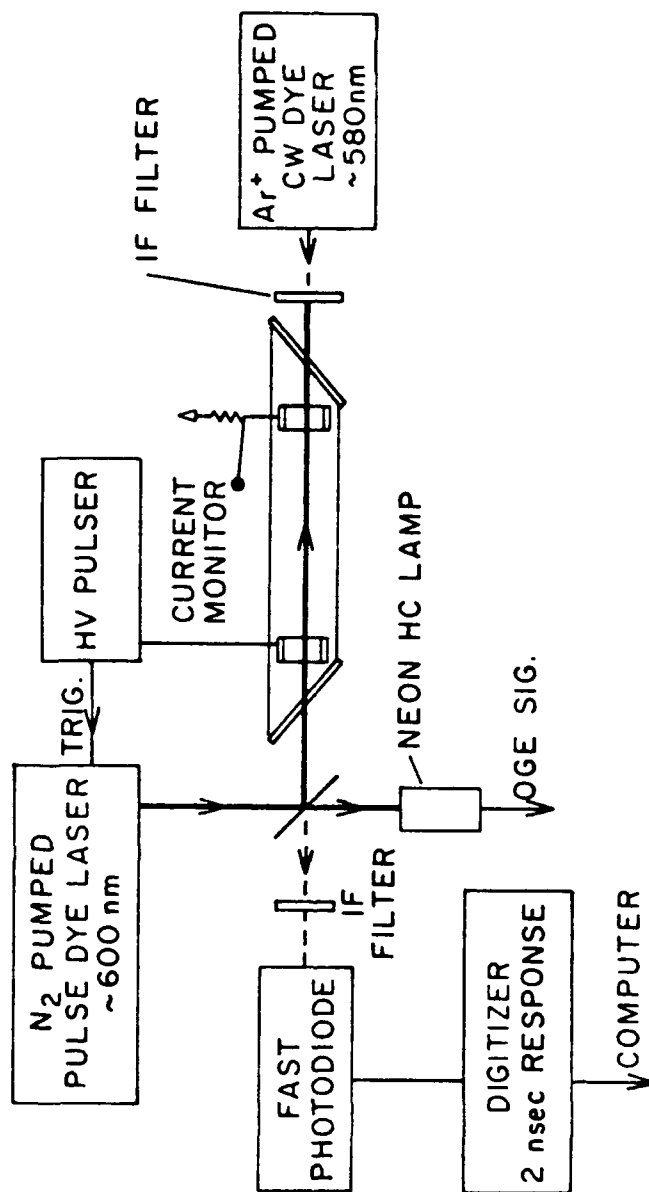


Figure 7. Schematic of apparatus used in high time resolution absorption measurements.

N_2 laser is triggered so as to provide a dye laser pulse after the discharge current and metastable density has reached a steady value. The resultant transient absorption wave form is shown in Fig. 8. For these discharge conditions the absorption during the discharge was about 2%, so that for our ratio of laser to Doppler linewidths the absorption is directly proportional to the $c^3\Pi_u$ density. For the pulsed dye laser conditions of 15 GHz linewidth and a pulse flux of 10 kW/cm^2 at the discharge the observed change in absorption corresponds to a $c^3\Pi_u$ metastable depletion of about 50% at a H_2 density of 10^{22} m^{-3} .

Our interest is in the recovery of population and therefore absorption following the dye laser pulse indicated by the central arrow in Fig. 8. In Fig. 9 this portion of the absorption waveform has been inverted and expanded in time. The smooth curve of Fig. 9 shows the fit of a simple exponential to this data. As discussed in Sec. IVE, we provisionally assume that the decay constant of this exponential is simply the collisional destruction frequency of the $c^3\Pi_u$ metastables by H_2 . We have measured such decay constants at H_2 densities from 1 to $3 \times 10^{22} \text{ molecules/m}^3$, but have not completed analysis of the data because of uncertainties in the system response, laser pulse width, etc. Preliminary indications are that the destruction rate coefficient required for consistency with these results is at least $2.2 \times 10^{-15} \text{ m}^3/\text{s}$. This is a very large value and corresponds to a quenching cross section of $90 \times 10^{-20} \text{ m}^2$. Such large values have been found for quenching of some singlet states of H_2 and for the $H_2 \text{ d}^3\Pi_u$ state.²¹

Many additional measurements are required before we can interpret this data with assurance. Some are:

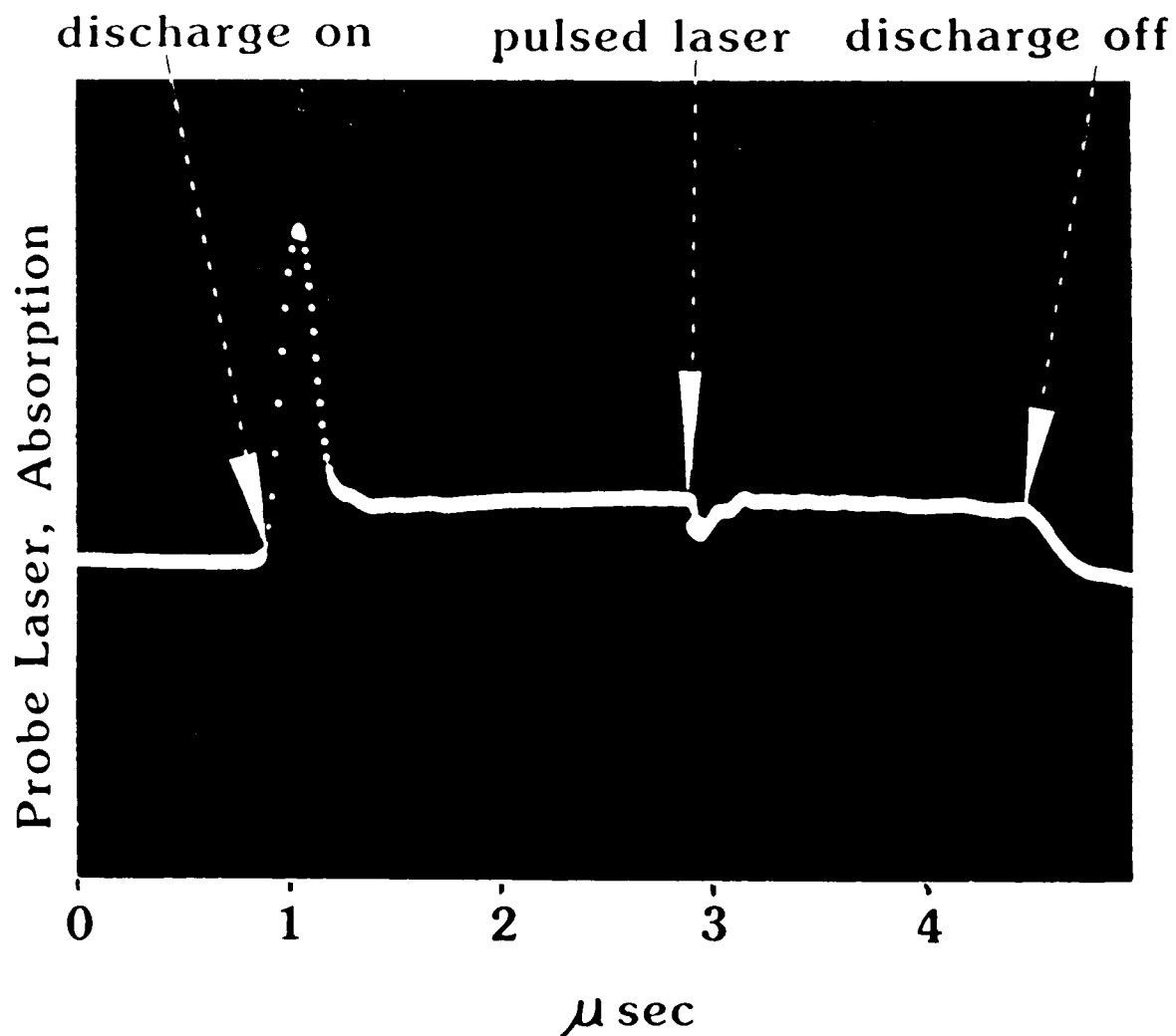


Figure 8. Overall transient absorption waveform showing effects during discharge pulse -- first and third arrows -- and metastable depletion caused by laser pulse -- center arrow.

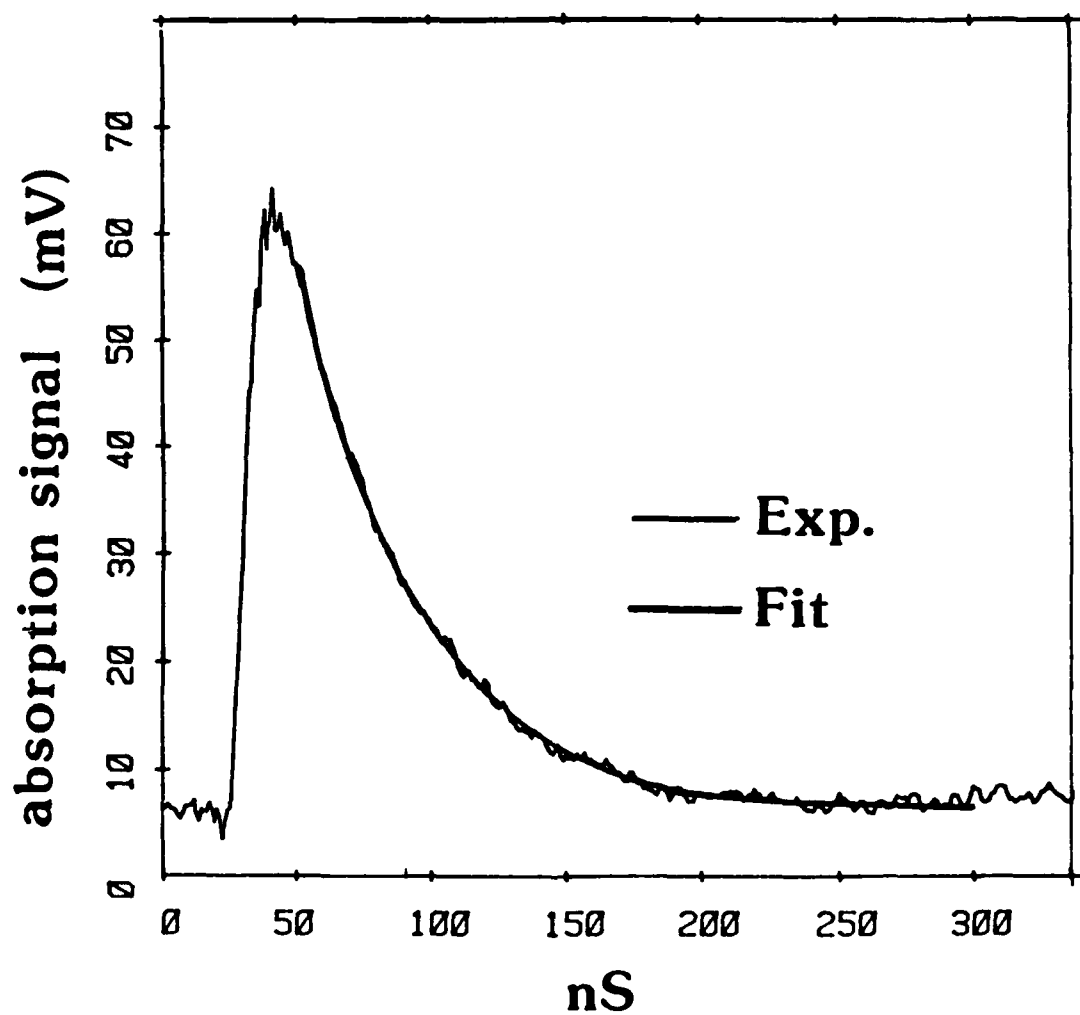


Figure 9. Expanded absorption waveform showing recovery of $c^3\pi_u$ ($N=1$, $v=2$) metastable population and exponential fit to data.

- measurements of the system time response;
- measurements of the dependence of the decay constants on discharge current and the intensities of the pulsed and cw dye lasers;
- measurements over a wider range of H_2 densities;
- observations of the changes in populations of nearby rotational, vibrational and electronic states which may be collisionally or radiatively coupled to the depleted level; and
- measurements of the decay constants for other rotational and vibrational levels of the H_2 $c^3\Pi_u$ state.

E. Models of H_2 excited state behavior

We have initiated the development of models of the transient behavior of the excited states of H_2 . In particular, we have examined solutions of the coupled rate equations describing the populations of the metastable and predissociating levels of the $c^3\Pi_u$ state and of the $a^3\Sigma_g^+$ state. Some of our results are shown in Fig. 10. Here the upper two curves show the two decay constants of the model, while the lower curve shows reciprocal of the normalized emission from the $a^3\Sigma$ state. The points associated with the lower curve are from our previous (AFWAL-TR-84-2017) measurements of the UV emission from the $a^3\Sigma$ state, while the square points are our preliminary data discussed in Sec. IVD. The solid curves are calculated neglecting collisional coupling, while the dashed curves are calculated with as large collision coupling rate coefficients as can be used while still fitting the emission data and while assuming forward and backward rate coefficients to be related by thermal equilibrium formulas. We conclude that with this limited model, collisional coupling of the $c^3\Pi$ and $a^3\Sigma$ states would be difficult to detect using the present measurements. These analyses bring out the importance of attempting

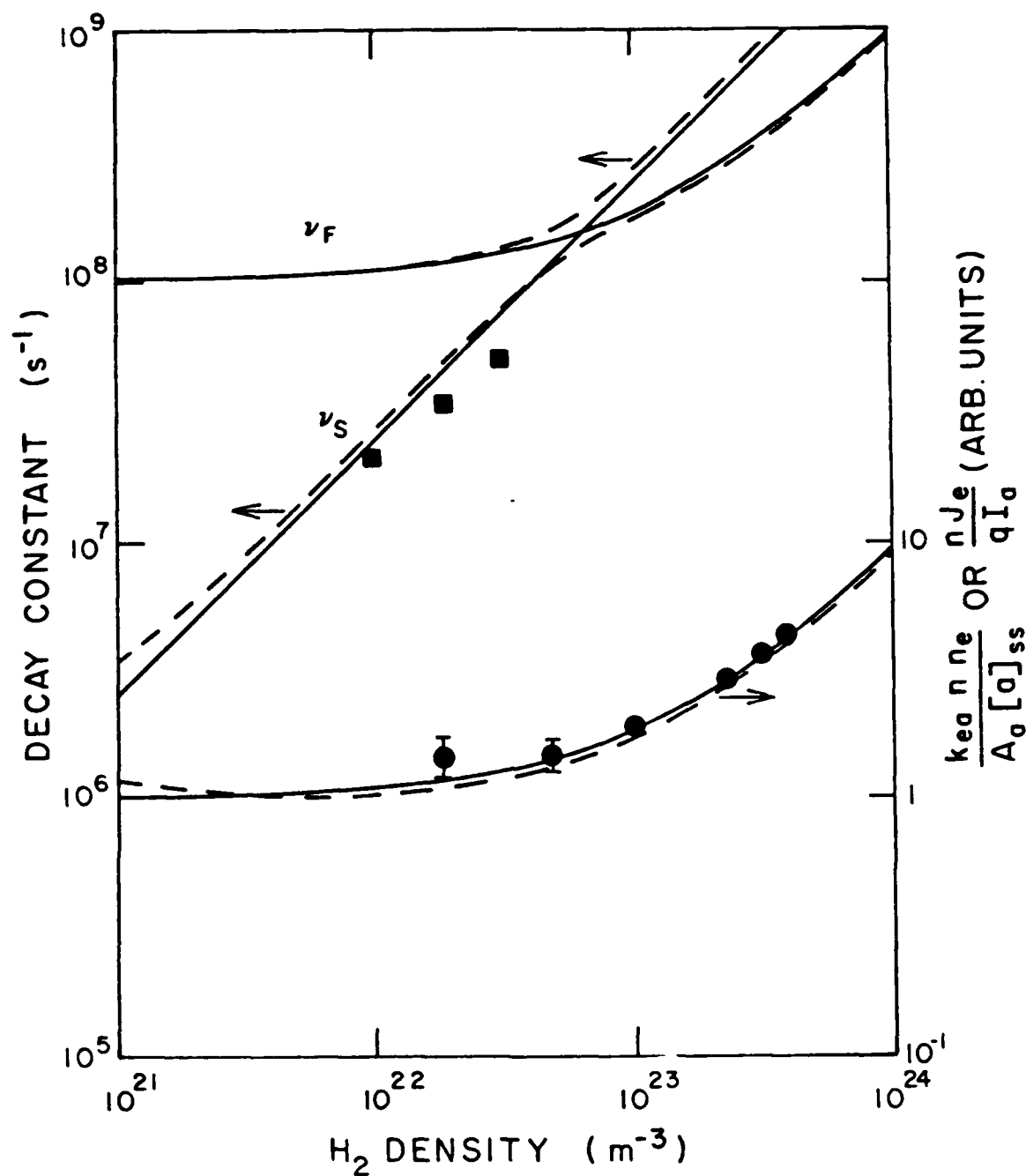


Figure 10. Decay constants (upper two curves) and relative amplitudes of UV emission (lower curve) for collisionally coupled $c^3\Pi_u$ and $a^3\Sigma_g^+$ states of H_2 . The solid lines are calculated neglecting collision coupling while the dashed line is calculated using the maximum collision rate coefficient consistent with the emission data shown by the circular points. The square points show our preliminary decay constant measurements.

to experimentally distinguish between collisional destruction of the $c^3\Pi_u$ state by a) excitation transfer to the $a^3\Sigma$ state, or b) rotational excitation to a predissociating level, or c) formation of a dissociating state¹¹ of H_4 . These considerations lead to the suggestion that one may be able to observe the depletion of the population of the $a^3\Sigma$ state when the c^3 density is depleted by the pulsed laser or vice versa.

The preliminary data analysis described in Sec. IVD is based on a simplified rate equation for the $c^3\Pi_u$ metastable population $M(t)$ in which we neglect any collisional or radiative transfer from other levels to the $c^3\Pi_u$ level. This equation is

$$\frac{dM(t)}{dt} = k_e n_e n - k_q n M(t) - \sigma \frac{\Gamma(t)}{h\nu} M(t) \quad (1)$$

where k_e is the rate coefficient for electron excitation of the $v''=2$, $N''=1$ level of the $c^3\Pi_u$ state, n_e is the electron density, n is the H_2 density, k_q is the total rate coefficient for collisional quenching of the metastables by H_2 , and σ is the effective cross section for absorption of the pump laser flux Γ and $h\nu$ is the photon energy. The solution of this equation after the laser pulse, i.e., for large enough t so that $\Gamma(t) = 0$, is

$$M = \frac{k_e n_e}{k_q} - \Delta M e^{-\nu t} \quad (2)$$

where the decay constant is given by $\nu = k_q n$ and ΔM is the change in the metastable density at the end of the laser pulse. The maximum in the metastable depletion is obtained by setting $dM/dt = 0$ in Eq. (1) to obtain

$$\Delta M_{\max} = \frac{k_e n_e \sigma \Gamma(t) / h\nu}{k_q [k_q n + \sigma \Gamma(t) / h\nu]} \quad (3)$$

Note that ΔM in Eqs. (2) and (3) are approximately equal but not identical.
Equation (3) is observed to be approximately obeyed in our experiments.

SECTION V

CONCLUSIONS

The results described in this report show that the properties of the metastable state of H_2 in electrical discharges in H_2 are much different than previously thought, i.e., the collisional lifetimes are very short. We have successfully adapted modern pulsed and cw dye laser techniques to the measurement of these lifetimes. We therefore recommended that these experiments be continued so as to determine the rate coefficients for the collisional destruction of the $c^3\Pi_u$ metastables and for any collisional coupling to nearby states of H_2 . These experiments should then be extended to determine the excitation coefficients for the $c^3\Pi_u$ state metastable state.

Future work should emphasize the application of the techniques developed to the diagnostics of discharges and the improvement of our ability to predict more accurately the characteristics of these discharges. An example is our plan to use measurements of excited state densities to test models of spatial development of parallel plane discharges in the presence of space charge effects and any ionization resulting from the presence of excited molecules.

Electrical discharges in molecular gases such as H_2 (D_2) are the subject of renewed interest because of their importance in devices such as high power switches, plasma processing cells and negative ion sources and because of the need for improved performance of these devices. The physical processes, such as metastable formation and quenching, being measured under this project for H_2 are also of importance in atmospheric gases where current interest is in charged particle beam propagation, lightning, etc. One question of importance in understanding and predicting the times characteristic of current switching in hydrogen thyratrons being answered by this research is the effective

lifetime of the metastable state of H_2 and the role of collisions which quench or ionize the metastables in the growth and decay of the electron density. Another question is the role of electronically excited states, such as the $c^3\Pi_u$ and $a^3\Sigma_g^+$ states, in the production of vibrationally excited H_2 in discharges used for the production of H^- ions.

REFERENCES

1. W. Lichten, J. Chem. Phys. 26, 306 (1957); Phys. Rev. 120, 848 (1960);
ibid. 126, 1020 (1962); P. R. Brooks, W. Lichten, and R. Reno, Phys. Rev.
A 4, 2217 (1971); W. Lichten and T. Wik, J. Chem. Phys. 69, 5428 (1978);
W. Lichten, T. Wik, and T. A. Miller, J. Chem. Phys. 71, 2441 (1979).
2. G. Herzberg, Science of Light 16, 14 (1967).
3. T. J. Morgan, K. H. Berkner, and R. V. Pyle, Phys. Rev. A 5, 1591 (1972).
4. C. E. Johnson, Phys. Rev. A 5, 1026 (1972); ibid. 9, 576 (1974).
5. M. Volger and B. Meierjohann, Phys. Rev. Letters 38, 57 (1977); B.
Meierjohann and M. Volger, Phys. Rev. A 17, 47 (1978).
6. E. E. Eyler and F. M. Pipkin, Phys. Rev. Lett. 47, 1270 (1981) and J.
Chem. Phys. 77, 5315 (1982).
7. D. P. DeBruijn, J. Neuteboom, V. Sidis, and J. Los, Chem. Phys. 85, 215
(1984); D. P. DeBruijn, J. Neuteboom, and J. Los, ibid., 85, 233 (1984);
H. Helm, D. P. DeBruijn, and J. Los, Phys. Rev. Lett. 53, 1642 (1984).
8. M. Glass-Maujean, J. Physique - Lettres 38, L-427 (1977).
9. L.-Y. Chow Chiu, J. Chem. Phys. 40, 2276 (1964); D. K. Bhattacharyya and
L.-Y. Chow Chiu, ibid. 67, 5727 (1977); L.-Y. Chow Chiu and D. K.
Bhattacharyya, ibid. 70, 4376 (1979).
10. R. P. Freis and J. R. Hiskes, Phys. Rev. A 2, 573 (1970).
11. W. Gerhartz, R. D. Poshusta, and J. Michl, J. Am. Chem. Soc. 98, 6427
(1976) and 99, 4263 (1976); J. D. Goddard and I. G. Csizmadia, Chem.
Phys. Lett. 43, 73 (1976) and 64, 219 (1979); M. Jungen and V. Staemmler,
Chem. Phys. Lett. 103, 191 (1983); C. A. Nicolaides, G. Theodorakopoulos,
and I. D. Petsalakis, J. Chem. Phys. 80, 1705 (1984).
12. H. M. Crosswhite, The Hydrogen Wavelength Tables of Gerhard Heinrich
Dieke (Wiley, New York, 1972).

13. D. S. Bethune, J. R. Lankard and P. P. Sorokin, J. Chem. Phys. 69, 2076 (1978).
14. J. R. Hiskes, A. M. Karo, M. Bacal, A. M. Bruneteau, and W. G. Graham, J. Appl. Phys. 53, 3469 (1982).
15. C. Bottcher and B. D. Buckley, J. Phys. B 12, L497 (1979).
16. M. Gundersen and S. Guha, J. Appl. Phys. 53, 1190 (1982); S. Guha, J. A. Kunc and M. A. Gundersen, IEEE J. Quantum Elect. QE-20, 504 (1984).
17. G. H. Herbig, Ap. J. 137, 200 (1963); J. M. Malville, Ap. J. 139, 198 (1964).
18. W. B. McKnight and T. A. Barr, Jr., Appl. Optics 21, 357 (1982); T. A. Barr Jr. and W. B. McKnight, Appl. Phys. Lett. 41, 114 (1982).
19. I. Dabrowski and G. Herzberg, Acta Phys. Hungar., submitted.
20. D. Feldman, Opt. Comm. 29, 67 (1979).
21. E. W. Fink, D. L. Akins, and C. B. Moore, J. Chem. Phys. 56, 900 (1972); J. Van der Linde and F. W. Dalby, Can. J. Phys. 50, 287 (1972); J. W. L. Lewis and W. D. Williams, J. Quant. Spectrosc. Radiat. Transfer 16, 939 (1976); A. Catherinot, B. Dubreuil, and M. Gand. Phys. Rev. A 18, 1097 (1978); B. Dubreuil and A. Catherinot, J. Physique 39, 1071 (1978); D. J. Kligler, J. Bokor, and C. K. Rhodes, Phys. Rev. A 21, 607 (1980).

END

FILMED

7-85

DTIC